

TARP-associated AMPA receptors display an increased maximum channel conductance and multiple kinetically distinct open states

Chris Shelley, Mark Farrant and Stuart G. Cull-Candy

Department of Neuroscience, Physiology, and Pharmacology, University College London, Gower Street, London WC1E 6BT, UK

Key points

- Signalling of information in the nervous system relies on the activation of specific neurotransmitter receptors.
- Here we characterise some of the properties of GluA1 AMPA receptors, whose ion-permeable channel is opened by the neurotransmitter glutamate.
- We found that the individual single-channel openings exhibit several discrete conductance levels that persist in the presence of saturating glutamate concentrations, and that the presence of modulatory accessory subunits differentially influences the durations of these channel openings.
- Our data also indicate that there are at least two kinetically distinguishable stable open states for each conductance level.
- These observations place constraints on models of GluA1 function that can be used to relate receptor properties to synaptic function.

Abstract Fast excitatory synaptic transmission in the CNS is mediated mainly by AMPA-type glutamate receptors (AMPA receptors), whose biophysical properties are dramatically modulated by the presence of transmembrane AMPAR regulatory proteins (TARPs). To help construct a kinetic model that will realistically describe native AMPAR/TARP function, we have examined the single-channel properties of homomeric GluA1 AMPARs in combination with the TARPs, γ -2, γ -4 and γ -5. In a saturating concentration of agonist, each of these AMPAR/TARP combinations gave rise to single-channel currents with multiple conductance levels that appeared intrinsic to the receptor-channel complex, and showed long-lived subconductance states. The open time and burst length distributions of the receptor complexes displayed multiple dwell-time components. In the case of γ -2- and γ -4-associated receptors, these distributions included a long-lived component lasting tens of milliseconds that was absent from both GluA1 alone and γ -5-associated receptors. The open time distributions for each conductance level required two dwell-time components, indicating that at each conductance level the channel occupies a minimum of two kinetically distinct open states. We have explored how these data place novel constraints on possible kinetic models of TARP-associated AMPARs that may be used to define AMPAR-mediated synaptic transmission.

(Resubmitted 31 May 2012; accepted after revision 13 September 2012; first published online 17 September 2012)

Corresponding authors M. Farrant and S. G. Cull-Candy: Department of Neuroscience, Physiology, and Pharmacology, University College London, Gower Street, London WC1E 6BT, UK. Email: s.cull-candy@ucl.ac.uk and m.farrant@ucl.ac.uk

Abbreviations AMPAR, AMPA receptor; CP-AMPA, calcium-permeable AMPA receptor; eGFP, enhanced green fluorescent protein; LBD, ligand-binding domain; TARP, transmembrane AMPA receptor regulatory protein.

Introduction

Central excitatory transmission is mediated mainly by AMPA-type glutamate receptors (AMPA receptors). The subunits forming these receptors (GluA1–4) function as homo- or heterotetramers (Traynelis *et al.* 2010), with biophysical and pharmacological properties, and interactions with intracellular signalling partners that depend critically on their subunit composition. Changes in the number and subtype of synaptic AMPARs have been shown to underlie many forms of synaptic plasticity, including long-term potentiation and depression (Malinow & Malenka, 2002; Shepherd & Huganir, 2007; Collingridge *et al.* 2009), a switch in postsynaptic calcium permeability (Liu & Cull-Candy, 2000; Cull-Candy *et al.* 2006; Liu & Zukin, 2007) and homeostatic scaling (Shepherd *et al.* 2006). The transmembrane AMPAR regulatory proteins (TARPs) are a major family of AMPAR auxiliary proteins (Jackson & Nicoll, 2011) that act to modulate the surface expression, pharmacology and biophysical properties of AMPARs, thereby shaping the time course of fast glutamatergic signalling in the brain. Co-expression of TARPs with AMPAR subunits in recombinant systems yields AMPARs with properties that closely mimic those of native AMPARs (Tomita *et al.* 2005; Soto *et al.* 2007). Based on their functional properties, TARPs fall into two groups, the more typical 'type I' TARPs (γ -2, γ -3, γ -4 and γ -8) and the atypical 'type II' TARPs (γ -5 and γ -7), which differ in their C-terminal tail length and their PDZ ligands.

Any realistic model of fast excitatory synaptic signalling in the CNS requires basic information about defined AMPAR/TARP complexes, including their functional properties and how these are regulated by TARPs. The rapid kinetics and complex brief openings of AMPAR channels tend to hamper the recording of well-resolved single-channel currents. However, homomeric calcium-permeable (CP-)AMPA receptors exhibit a relatively large conductance, compared with their calcium-impermeable counterparts (Swanson *et al.* 1997). While it is known that their channel conductance is further increased, and channel kinetics slowed, when these CP-AMPA receptors are co-assembled with TARPs (Tomita *et al.* 2005; Soto *et al.* 2009), the basic mechanisms underlying these effects are poorly defined. For example, it is unclear whether all TARPs act to increase the maximum conductance state of AMPAR channels, or if they merely alter the relative probability of opening to the different pre-existing conductance levels.

Here we have examined the properties of homomeric GluA1 receptors, alone and in combination with three different TARPs: γ -2, γ -4 and γ -5. Stargazin (γ -2), the prototypical TARP, is widely expressed in the brain, with particularly high levels in cerebellar neurons. TARPs γ -4 and -5 are also found in many brain regions, including the cerebellum and hippocampus (Green *et al.* 2001;

Tomita *et al.* 2003; Fukaya *et al.* 2005). We found that each of the TARPs examined increased GluA1 mean single-channel conductance. Unexpectedly, this could be ascribed to an approximate doubling of each of the multiple conductance levels. This contrasts with the mechanism previously described for GluA4 receptors, in which associated TARPs did not affect the conductance of the single-channel openings, but instead increased the relative proportion of higher conductance events (Tomita *et al.* 2005). In addition, we found that TARP-associated AMPARs can adopt many more open states than was previously envisaged – a feature that places constraints on kinetic models of AMPAR/TARP function.

Methods

Heterologous expression

tsA201 cells were maintained in culture as described previously (Soto *et al.* 2007). Cells were transiently transfected with GluA1 flip isoform and TARP cDNA at a ratio of 1:3, using Lipofectamine (Invitrogen, Paisley, UK). A GluA1/ γ -4 fusion protein was constructed by inserting a GluA1-encoding cDNA fragment into a pIRES vector containing a γ -4-encoding region, via NheI and EcoRI sites. The resulting linker sequence of GGGGGEFAT between GluA1 and γ -4, and the removal of the GluA1 stop codon were confirmed by DNA sequencing. Enhanced green fluorescent protein (eGFP) cDNA was also included to allow subsequent visualisation of successfully transfected cells. Cells were passaged and plated onto glass coverslips 16–18 h after transfections, and recordings were made after a further 48–80 h. Rat TARP cDNAs were gifts from R. Nicoll (UCSF).

Electrophysiological recordings

Borosilicate glass pipettes (1.5 mm o.d., 0.86 mm i.d.; Harvard Apparatus, Edenbridge, UK) were pulled to give resistances of 8–12 M Ω and their tips coated with Sylgard. Cells were visualised on an upright Zeiss Axioskop microscope with a 40 \times immersion objective. Recordings were made at room temperature using an Axopatch 200A and a CV201A headstage (Molecular Devices, Sunnyvale, CA, USA). Outside-out patches were pulled from eGFP-positive cells and voltage-clamped at -80 mV. The external bath solution contained (in mM): NaCl, 145; KCl, 2.5; CaCl₂, 1; MgCl₂, 1; Hepes, 10; glucose, 10 (pH 7.3 with NaOH); and glutamate, 10 where specified. The internal (pipette) solution contained (in mM): CsCl, 145; NaCl, 2.5; EGTA-Cs, 1; Mg-ATP, 4; Hepes, 10 (pH 7.3 with CsOH). Most data were acquired online – low-pass filtered at 10 kHz and sampled at 50 kHz (Digidata 1322A, Molecular Devices, Sunnyvale, CA, USA). In some cases

currents were recorded onto digital audio tape (DTR-1205 recorder; Biologic, Claix, France); in these cases data were filtered at 5 kHz during re-digitisation.

Single-channel analysis

For analysis, data were further filtered at 1 kHz giving a total filtering of 0.976–0.995 kHz. Although this high filtering leads to an overestimate of apparent open times, it was used in order to improve the signal-to-noise ratio, allowing the unambiguous identification of channel sublevels. Events amplitudes and durations were measured using the SCAN program (<http://ucl.ac.uk/Pharmacology/dcpr95.html>). The transitions were fitted with convolved step-response functions using a least-squares criterion (Colquhoun & Sigworth, 1995). Following idealisation, a conservative resolution of 664 μ s was imposed. The mean number of events fitted for each patch was 1665 ± 303 , $n = 33$. Amplitude histograms were fitted with two–four Gaussian components, using maximum likelihood. The most appropriate number of components to fit to the amplitude histograms was determined by fitting increasing numbers of Gaussian components until there was no significant increase in the likelihood value. As the natural log likelihood ratio between two fits is distributed as χ^2 (McManus & Magleby, 1988), and an additional Gaussian component in a fit adds an extra three free parameters, log likelihood ratios greater than 7.82 were judged significant, at the $P = 0.05$ level. For classifying open levels, A_{crit} values were calculated using the criteria of equal percentages of lower and higher amplitude events being misclassified. Open periods, shut times and burst property histograms were fitted with a mixture of exponential components using the EKDIST program. To define bursts, a t_{crit} value was calculated so as to ensure an equal proportion of intervals from the lower and higher components were misclassified (Colquhoun & Sakmann, 1985), typically the two fastest closed time components were deemed to be within bursts. Overall mean values of single-channel conductance, open periods and burst lengths were calculated as the mean of the weighted mean values for each individual patch, rather than the weighted mean of the mean component values given in the tables. Durations and relative occupancies of the different open channel conductance levels were extracted from the idealised data using custom programs written with Scilab 5.0.2 (<http://www.scilab.org>). Significant differences in the means of multiple comparison data were assessed with one-way ANOVA (Welch's heteroscedastic F -test), followed by pairwise comparisons using Welch two-sample t tests (with Holm's sequential Bonferroni correction for multiple comparisons). These tests were performed using R (version 2.14.1, The R Foundation for Statistical Computing; <http://www.R-project.org>) and RStudio

(version 0.96.36, RStudio, Inc., <http://rstudio.org/>). Significance of correlations was assessed with Spearman rank order correlation tests (Origin Pro 8.5, OriginLab Corporation, Northampton, USA). For all tests $P < 0.05$ was considered significant.

Results

TARP-associated AMPAR channels exhibit multiple conductance states

Figure 1A shows examples of single-channel currents activated by a saturating concentration of glutamate (10 mM), approximately 500-fold greater than the glutamate EC_{50} (Kott *et al.* 2007), in outside-out patches from cells expressing GluA1 alone, or GluA1 with γ -2, γ -4 or γ -5. As receptors are desensitised in these conditions, the bursts of openings observed are likely to arise from individual channels that transiently escape from the desensitised state(s). We noted that all of the AMPAR complexes examined exhibited multiple conductance states, both with and without TARPs. In addition, there was variability in the number of discrete conductance states observed for each type of AMPAR/TARP complex.

Amplitude histograms from GluA1 alone, GluA1/ γ -2 and GluA1/ γ -5 were best fitted with either two or three Gaussian components, whilst amplitude histograms from GluA1/ γ -4 AMPARs were best fitted with two–four components. Examples from different patches are shown in Fig. 1B, and the mean amplitudes derived from the fitted Gaussians are summarised in Fig. 2 and Table 1.

Variability in number of multiple conductance states

To determine if variability in the amplitude distributions reflected intrinsic differences between receptors, or differences in the duration or quality of recordings obtained from individual patches, we plotted the number of significant amplitude components detected against the number of events fitted, or against the root mean squared (r.m.s.) noise of individual patches. In both cases, we found no correlation (Fig. 3), suggesting that variability was a genuine feature of the TARP-associated receptors. The absence of third and fourth conductance components in some of the conductance distributions could be due to unresolved low-amplitude events, unresolved brief openings or differences in intrinsic channel properties (such as 'moding'). Moding, which has previously been observed in other glutamate receptor ion channels (Popescu & Auerbach, 2003; Poon *et al.* 2010), is the abrupt change in channel properties seen under steady-state conditions, often involving a change in open probability. A one-way between-subjects ANOVA was conducted to compare the effect of TARP status on single-channel conductance of GluA1

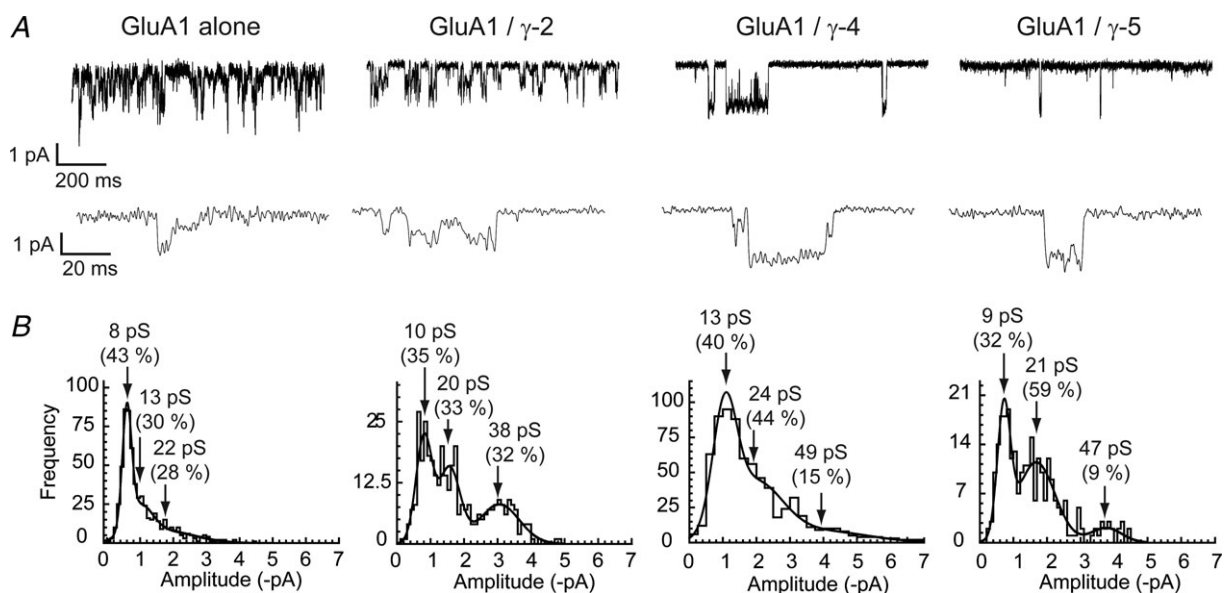
Table 1. Mean, SEM and *n* number values for fits to conductance histograms for homomeric GluA1 receptors with and without TARPs

TARP	Single-channel conductance (pS)	Conductance level (pS) + (percentage area of component)			
		1	2	3	4
None	13.7 ± 0.8 <i>n</i> = 5	7.6 ± 0.9 (35 ± 5)	12.9 ± 0.3 (73 ± 15)	24.8 ± 3.9 (34 ± 15)	—
γ -2	27.6 ± 3.4* <i>n</i> = 8	11.5 ± 1.2* (32 ± 8)	22.3 ± 2.6*** (38 ± 8)	38.8 ± 2.8* (42 ± 11)	—
γ -4	26.4 ± 3.5* <i>n</i> = 11	12.3 ± 1.4* (47 ± 7)	22.9 ± 1.3*** (33 ± 7)	42.3 ± 3.6* (37 ± 8)	57.2 ± 5.3 (9 ± 2)
γ -5	20.8 ± 1.1* <i>n</i> = 6	9.4 ± 0.3 (32 ± 4)	21.7 ± 0.7 (61 ± 3)	38.1 ± 2.5 (20 ± 4)	—

In the case of single-channel conductance, *n* refers to the number of patches. For the statistical analysis of mean conductance (column 2), all TARPs were included. For the statistical analysis of the individual conductance levels, γ -5 was excluded (italics) because of the low number of events (<100) within several of the individual conductance components, and because of the low number of patches containing conductance levels 1 and 3 (4 in each case) compared with the other TARPs. *F*-tests denote results of one-way ANOVA (Welch's heteroscedastic *F*-test) and asterisks denote results of *post hoc* tests comparing GluA1 with GluA1/ γ -2 and GluA1/ γ -4 (Welch *t* tests with Holm's sequential Bonferroni correction; ****P* < 0.001, **P* < 0.05). $F_{3,12.62} = 9.26$, $F_{2,7.96} = 5.04$, $F_{2,10.43} = 34.25$, $F_{2,6.75} = 5.45$. *P* = 0.0017, *P* = 0.039, *P* = 2.61e-05, *P* = 0.038.

AMPA receptors: GluA1 alone, GluA1 + TARPs γ -2, γ -4 or γ -5. There was a significant effect of TARP status on single-channel conductance at the *P* < 0.05 level for the four groups ($F_{3,12.62} = 9.264$, *P* = 0.0017). *Post hoc*

pairwise comparisons using Welch two-sample *t* tests indicated that the mean conductance for GluA1 alone (13.7 ± 0.83 , *n* = 5) was significantly different from that seen with TARP γ -2 (27.6 ± 3.4 , *n* = 8; *P* = 0.013), γ -4

**Figure 1. GluA1 receptors with- and without TARPs open to multiple conductance levels**

A, single-channel currents recorded from GluA1 co-expressed with a TARP (γ -2, γ -4 or γ -5, as indicated). Outside-out patches were held at -80 mV; openings in the presence of 10 mM glutamate are shown as downward deflections and are illustrated at two different time scales. B, all TARPs tested exhibited multiple single-channel conductance levels. Amplitude histograms of single-channel events from individual patches fitted with multiple Gaussian components (see Methods). The mean conductances of the displayed distributions (and their relative areas) are indicated by arrows.

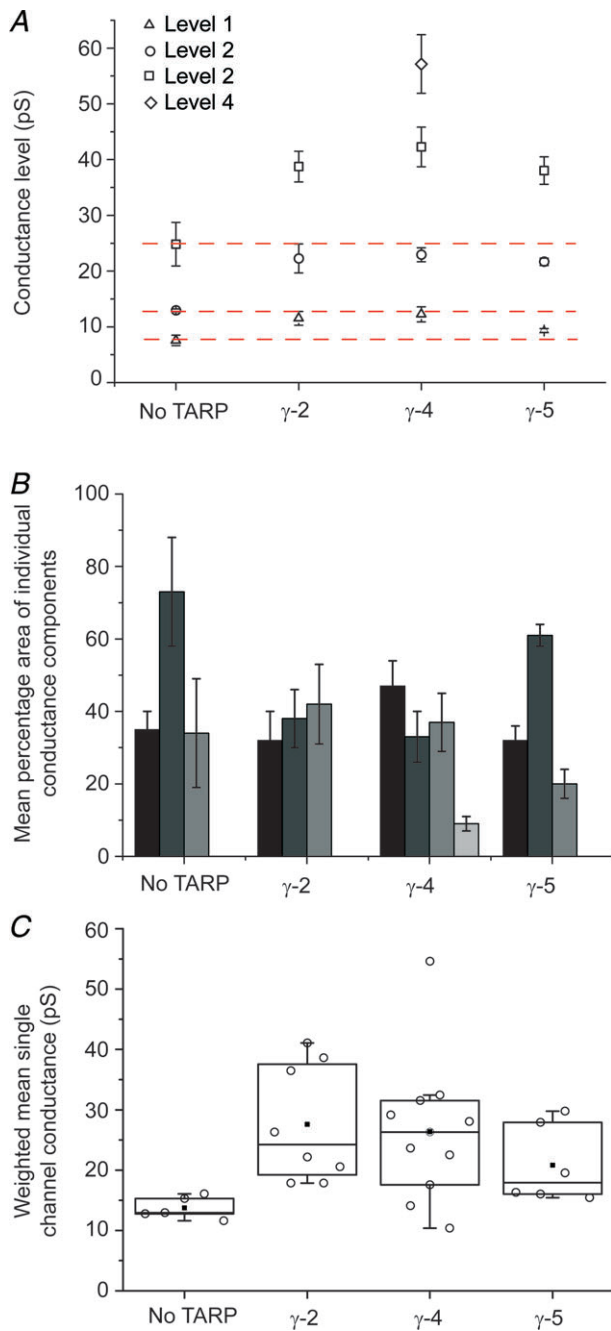


Figure 2. Parameters of fits to conductance histograms for homomeric GluA1 receptors with- and without TARPs

A, mean amplitudes of sub- and maximum conductance levels obtained from fitted amplitude distributions (error bars denote SEM). GluA1 alone, γ -2 and γ -5 complexes could be fitted with up to three components, whilst γ -4 complexes could be fitted with up to four components. The red dotted lines indicate the conductance levels for GluA1 without a TARP for comparison with GluA1 with TARP. *B*, mean areas of the conductance components shown in *A*. *C*, weighted mean single-channel conductance values of GluA1 alone ($n = 5$) and co-expressed with γ -2 ($n = 8$), γ -4 ($n = 11$) or γ -5 ($n = 6$). In the box-and-whisker plots, the top and bottom of the boxes are 25th and 75th percentiles, and the centre line is the 50th percentile (median). The whiskers extend to the first points before the ‘outlier’ cut-offs ($<Q1 - 1.5 \times IQR$ or $>Q3 + 1.5 \times IQR$). Parameters

(26.4 ± 3.5 , $n = 11$; $P = 0.013$) or γ -5 (20.8 ± 2.6 , $n = 6$; $P = 0.041$). There were no significance differences in the mean conductance between the different TARPs (Fig. 2*C*; Table 1).

To characterise the channel activation of the GluA1/TARP assemblies, we constructed dwell-time distributions of all open events (irrespective of conductance), and fitted these with multiple component

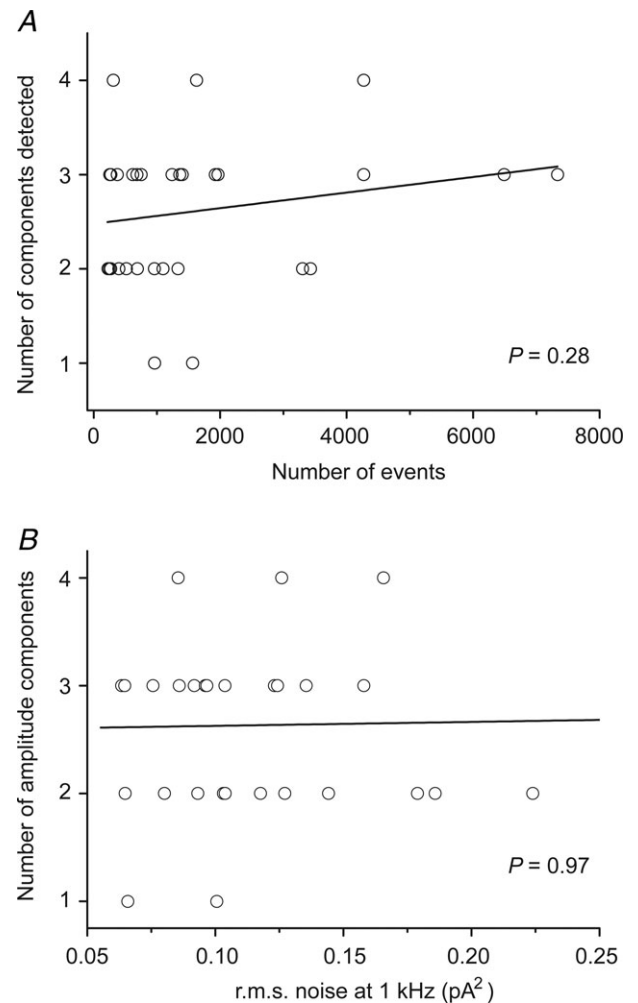


Figure 3. Variability in the number of events recorded and the baseline noise of each patch did not influence the number of conductance components detected

A, there was no correlation between the number of conductance components detected and the number of events analysed, indicating that the number of events was not a limiting factor in accurately detecting the number of conductance components. *B*, there was no correlation between baseline noise of patches and the number of conductance components detected. r.m.s., root mean square.

are presented in Table 1 and the Results section. All of the GluA1/TARP complexes had significantly higher weighted mean single-channel conductance compared with GluA1 alone.

exponentials. Examples are shown in Fig. 4 and the mean parameters are listed in Table 2. GluA1 alone and GluA1/ γ -5 receptors showed a tendency toward slightly shorter mean open times, although these differences

were not significant. The open time distributions of GluA1/ γ -2 and GluA1/ γ -4 both required three exponential components to provide an adequate fit. However, GluA1 alone and GluA1/ γ -5 receptors

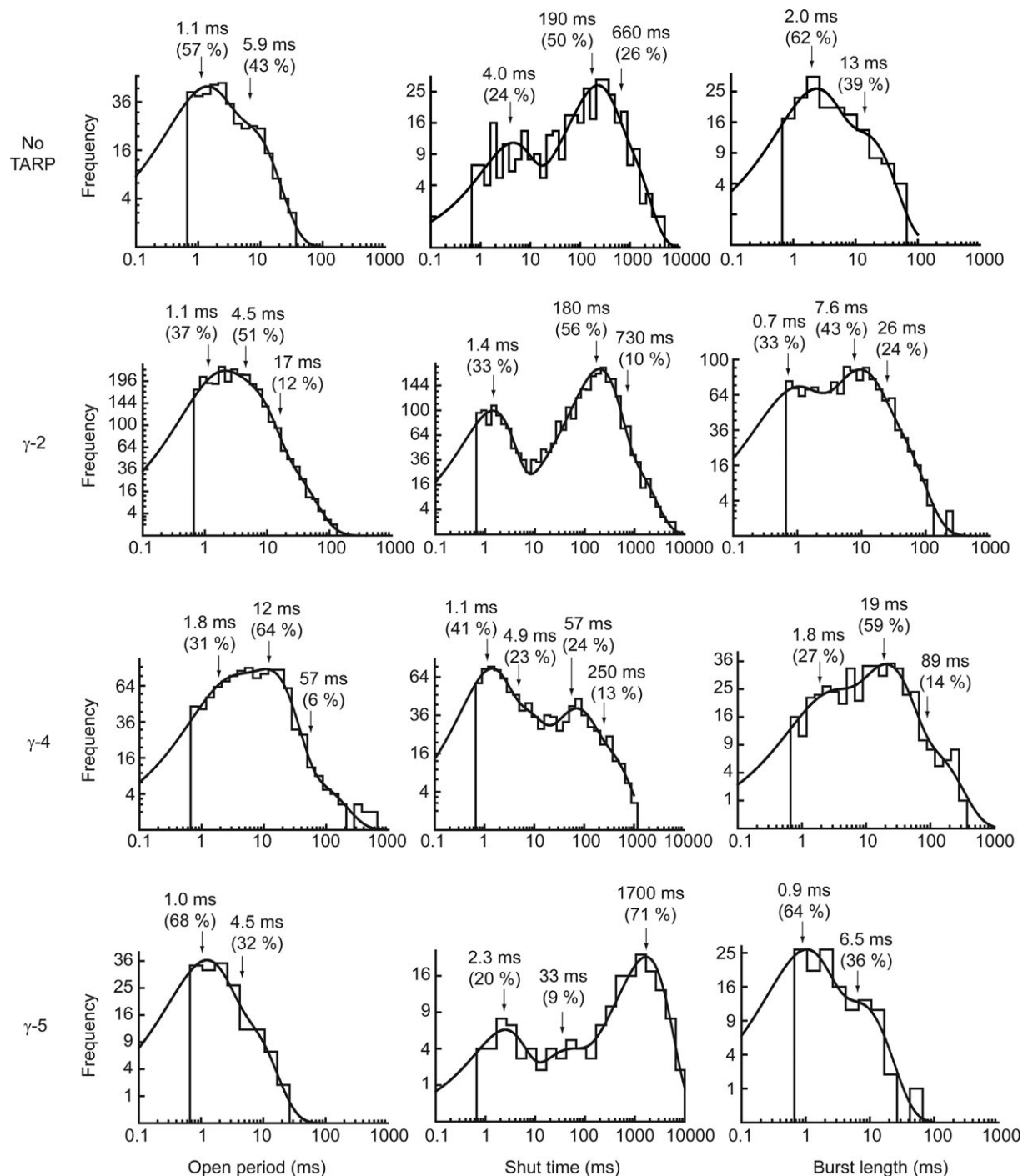


Figure 4. Representative single patch open period, shut time, and burst length dwell-time distributions for GluA1 alone and co-expressed with γ -2, γ -4 or γ -5 (see Methods)

When compared with GluA1 alone and GluA1/ γ -5, both GluA1/ γ -2 and γ -4 demonstrated a third long-lived time component in both the open period distributions and the burst length distributions.

Table 2. Mean and SEM values for parameters of fits to open period histograms for homomeric GluA1 receptors with different TARPs

TARP	Overall mean open period (ms)	Open period time constants (ms)		
		τ_1	τ_2	τ_3
None	4.2 ± 1.0 <i>n</i> = 5	1.7 ± 0.3 (64 ± 13)	16.1 ± 7.4 (36 ± 13)	—
γ -2	4.9 ± 0.5 <i>n</i> = 8	2.0 ± 0.5 (61 ± 9)	6.7 ± 1.2 (51 ± 10)	63.7 ± 20.1 (5 ± 3)
γ -4	9.4 ± 3.2 <i>n</i> = 11	1.0 ± 0.2 (51 ± 7)	5.9 ± 1.3 (51 ± 7)	45.1 ± 9.0 (14 ± 5)
γ -5	3.9 ± 1.4 <i>n</i> = 6	1.9 ± 0.5 (66 ± 8)	9.6 ± 4.3 (34 ± 8)	—

One-way ANOVA revealed no significant difference in the overall mean open periods between the four conditions ($F_{3,11,11} = 0.83$, $P = 0.50$) (Welch's heteroscedastic *F*-test).

required only two components, lacking the much longer component (with means of 64 ms and 45 ms) seen with the other TARPs. Given the resolution imposed during the fitting of individual openings, these values likely represent 'apparent' rather than true open times. However, it is clear from these data that TARPed GluA1 AMPARs have similar mean apparent open times regardless of whether they are co-expressed with γ -2, γ -4 or γ -5.

TARP subtypes give rise to channels with different burst length distributions

Measured burst lengths are much less sensitive than open periods to the imposed resolution. This is because undetected short shut times have minimal effects on overall burst length. To identify bursts of openings, shut time distributions (Fig. 4; Table 3) were constructed to enable the calculation of t_{crit} values. Bursts were defined as a sequence of openings and closings that ended once a shut time longer than t_{crit} had occurred. Burst length distributions, and their mean parameters, are shown in Fig. 4 and Table 4. As expected, given the imposed resolution, the burst length distributions resemble lengthened open period distributions. There was no significant difference in the mean burst length distribution of GluA1 AMPARs when associated with different TARPs. However, as with the open time distributions, GluA1 receptors in the absence of TARPs and GluA1/ γ -5 receptors required only two components to describe their burst length distribution, whereas GluA1 receptors in combination with both GluA1/ γ -2 and GluA1/ γ -4 required an additional long-lived component (with a mean of 58 ms and 154 ms, for γ -2- and γ -4-containing receptors, respectively).

TARP-associated AMPAR subunits display independent gating and multiple open states

To investigate the properties of the multiple conductance states in more detail, we focussed on GluA1/ γ -4 receptors as these produced the longest bursts of openings. Figure 5 shows example bursts, illustrating the range of conductance levels seen. Direct transitions were observed between all conductance levels, and between these and the baseline, suggesting that the sublevels observed represent different conductance states of the same channel, rather than reflecting the presence of several different types of channel within a patch. We also noted that sublevels could be relatively long-lived, extending to many milliseconds.

As described above, heterogeneity was apparent in the number of amplitude components detected within individual patches. Figure 6 shows examples of the heterogeneity obtained in patches from cells expressing GluA1/ γ -4. Heterogeneity in single-channel amplitude distributions from supposedly identical receptors could arise from variable GluA1/TARP stoichiometry in our heterologous expression system. To fix the GluA1/TARP stoichiometry at 1:1 stoichiometry (i.e. four TARPs per tetrameric receptor), we constructed a fusion protein consisting of GluA1 connected by a short linker to TARP γ -4 and recorded single-channel currents from HEK cells expressing this protein. Example currents and amplitude histograms from three separate patches are shown in Fig. 7. Clear single channels could be resolved, indicating that the construct was successfully folded and transported to the cell surface. However, as was the case with co-expression of GluA1 and γ -4, there was variability in the amplitude histograms obtained from several different patches. There was no significant difference in the weighted mean conductances for GluA1/ γ -4 (26.4 ± 3.5 , $n = 11$) and the

Table 3. Mean and SEM values for parameters of fits to shut time histograms for homomeric GluA1 receptors with different TARPs

TARP	n	Shut time constants (ms)			
		τ_1	τ_2	τ_3	τ_4
None	5	3.7 ± 1.0 (32 ± 6)	108.9 ± 20.5 (62 ± 6)	654.8 (26)	—
γ -2	8	1.4 ± 0.2 (23 ± 4)	6.4 ± 2.4 (20 ± 5)	98.1 ± 27.7 (72 ± 8)	326.4 ± 203.5 (19 ± 12)
γ -4	11	2.0 ± 0.5 (41 ± 4)	10.9 ± 1.8 (28 ± 4)	91.0 ± 12.3 (27 ± 5)	1090.8 ± 246.3 (18 ± 5)
γ -5	6	2.0 ± 0.2 (24 ± 4)	—	65.7 ± 15.0 (46 ± 11)	1419.3 ± 607.5 (45 ± 13)

Table 4. Mean and SEM values for parameters of fits to burst length histograms for homomeric GluA1 receptors with different TARPs

TARP	Overall mean burst length (ms)	Burst length time constants (ms)		
		τ_1	τ_2	τ_3
None	7.3 ± 1.5 n = 5	2.0 ± 0.4 (64 ± 14)	20.7 ± 10.0 (49 ± 17)	—
γ -2	6.7 ± 0.8 n = 8	1.1 ± 0.4 (42 ± 11)	6.6 ± 0.9 (78 ± 8)	58.2 ± 15.4 (11 ± 5)
γ -4	21.1 ± 5.3 n = 10	2.8 ± 1.0 (54 ± 4)	26.4 ± 5.0 (40 ± 3)	153.6 ± 44.7 (13 ± 6)
γ -5	8.1 ± 4.2 n = 6	1.3 ± 0.6 (52 ± 9)	11.4 ± 5.2 (56 ± 12)	—

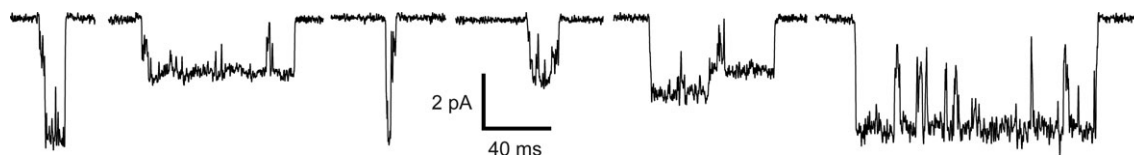
One-way ANOVA revealed no significant difference in the overall mean burst length between the four conditions ($F_{3,10,95} = 2.13$, $P = 0.16$; Welch's heteroscedastic F -test).

GluA1- γ -4 fusion protein (19.8 ± 4.7 , $n = 3$; Student's t test, $P = 0.30$).

Because of the heterogeneity in amplitude histograms, we focused on the GluA1/ γ -4 data sets labelled (A), (B) and (C) in Fig. 6, which displayed similar amplitude distributions. The single-channel data from these three patches were pooled. The resultant histogram showed four significant components (Fig. 8A), with mean conductances (and % areas) of 12 pS (30%), 19 pS (30%), 31 pS (26%) and 53 pS (15%), giving an overall weighted mean single-channel conductance of 25 pS. The pooled open time histogram from these patches was fitted with

four components, with an overall mean open time of 1.8 ms. The pooled burst length distribution (Fig. 8B) was well fitted with three components, with an overall mean burst length of 12.2 ms.

We found no significant correlation ($P = 0.20$) between the various conductance levels, and the mean open period duration of events at each conductance level (Fig. 8C). Thus, the duration of open times (and, by definition, the stability of the state) appeared to be independent of its conductance. Inspection of the distributions of open dwell-times of each of the conductance levels indicated that at least two exponential components were

**Figure 5. Typical single-channel currents from GluA1/ γ -4 assemblies, showing the presence of multiple conductance levels and long-lived subconductance states**

Currents are from the same patch held at -80 mV in the presence of 10 mM glutamate.

required to fit satisfactorily the open period histogram for each level (Fig. 8D). The mean value of the two open period dwell-time components was similar for each of the four conductance levels ($\tau_1 = 0.99 \pm 0.08$ ms, $\tau_2 = 5.23 \pm 0.59$ ms). This suggests that a minimum of two open states contribute to each of the four conductance levels, which indicates that a minimum of eight open states would be required in a full kinetic model of GluA1/ γ -4 receptors.

As the values measured for the open dwell-times were 'apparent' open times, due to the imposed resolution and filtering (1 kHz), we also examined single-channel

currents filtered less heavily (4.5 kHz). Figure 8E shows an example of an opening in which the long duration apparent openings detected with 1 kHz filtering are clearly interspersed with brief shuntings when the record was less filtered. Therefore, the mean value of the open time components for individual levels was almost certainly overestimated. However, this does not invalidate our finding that each conductance-specific open time distribution consists of multiple components. The multiple open time components for each conductance state could be artefactual if each conductance state open time histogram contained a significant proportion of

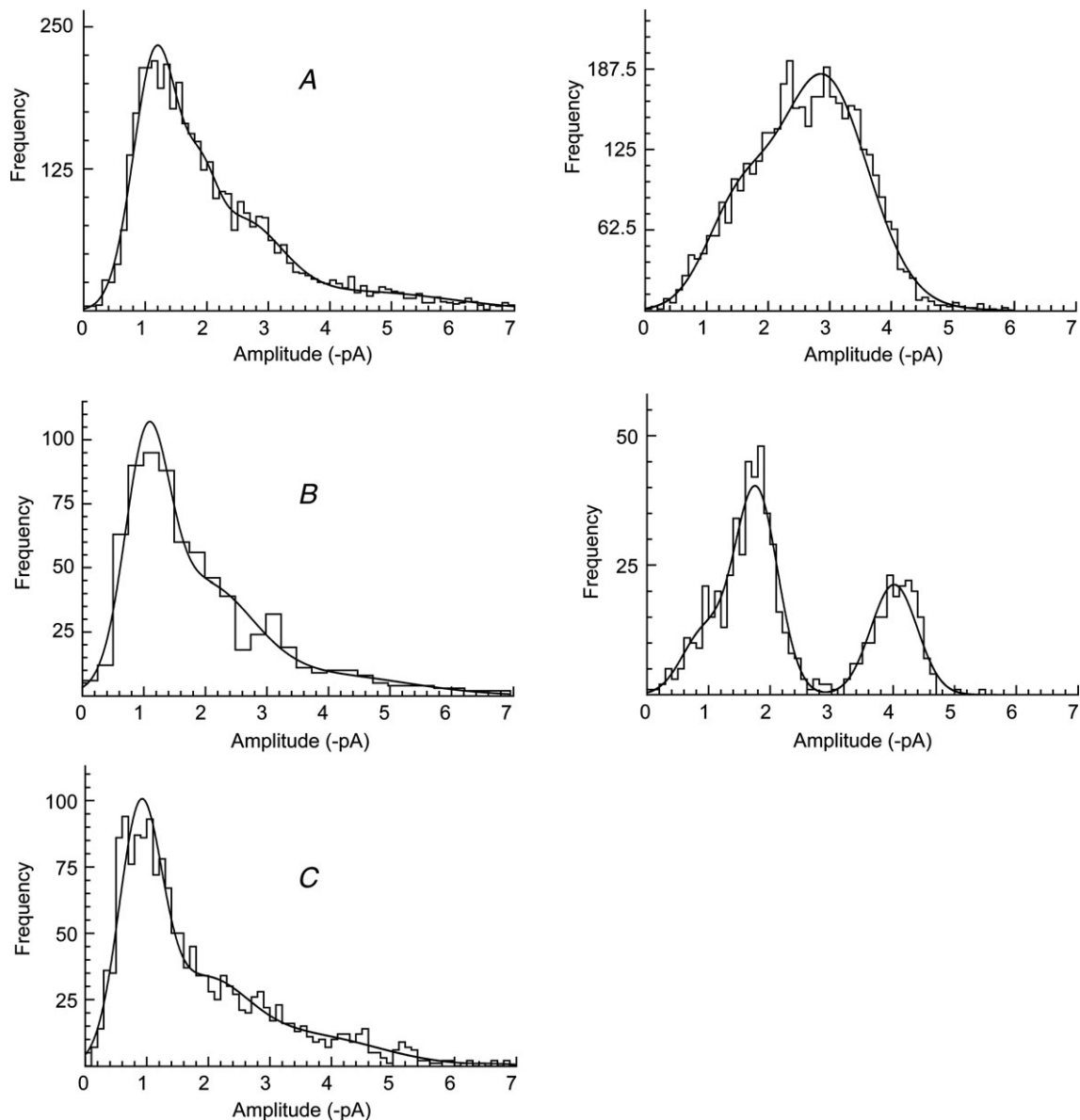


Figure 6. Typical amplitude histograms of single-channel currents recorded from patches excised from cells co-expressing GluA1 and γ -4

Note the heterogeneity in the single-channel amplitude distributions across patches. Data from (A), (B) and (C) were pooled for further analysis (in Fig. 7).

events from more than one conductance state. This could arise from the unavoidable misclassification of some amplitude events due to the overlap in the amplitude distributions (Fig. 8A). However, we found this was not the case, as the proportion of short- and long open times remained reasonably constant over all four of the conductance states, whereas the proportions would be expected to change dramatically if the two open time components arose from misclassified events.

It has been suggested that the individual AMPAR subunits within an assembly can gate independently (Prieto & Wollmuth, 2010; Kristensen *et al.* 2011). If this is indeed the case, then the frequency of the sojourns to the various conductance states is expected to be binomially distributed. Figure 9A shows the relative occupancy of the four open states, measured directly from the GluA1/ γ -4 pooled single-channel data. Assuming that individual subunits gate independently, the probability that a glutamate-bound subunit will gate the ion channel pore (coupling efficiency) can be estimated from the mean single-channel conductance. Figure 9B shows the predicted conductance level occupancy for all possible coupling efficiency values. For all such values, the predicted mean single-channel conductance was plotted

using the sublevel conductance values in Fig. 8A. From the fitted amplitude histogram we estimated a mean single-channel conductance of 24.7 pS, which corresponds to a coupling efficiency of 0.56 (Fig. 9C). The predicted subunit occupancy, for a coupling efficiency of 0.56, is plotted in Fig. 9A. It can be seen that our measured relative occupancy of channel conductance levels approximated well to those predicted for subunits that gate independently.

Discussion

Most fast excitatory synaptic transmission in the brain is mediated by AMPARs associated either with TARPs (Menuz *et al.* 2008) or other transmembrane proteins (Schwenk *et al.* 2009; von Engelhardt *et al.* 2010), or both (Gill *et al.* 2012; Schwenk *et al.* 2012). Although considerable information is available on single AMPAR channels, much of this has been obtained from recombinant receptors lacking auxiliary subunits. It is thus desirable to understand the channel gating of AMPARs co-assembled with auxiliary subunits, to reveal how their basic properties shape fast synaptic transmission.

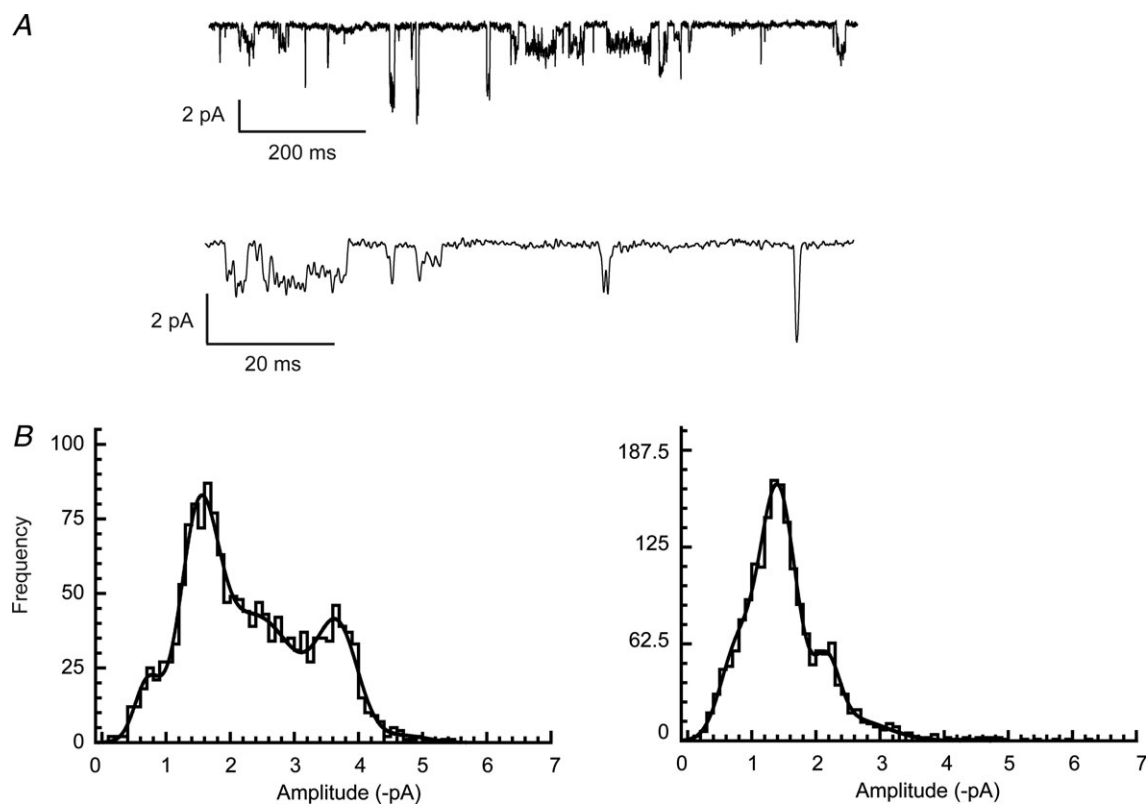


Figure 7. GluA1- γ -4 fusion proteins display multiple, heterogeneous conductance levels

A, single channels recorded from cells expressing GluA1- γ -4 fusion proteins. As with the subunits expressed separately, multiple conductance levels were observed. B, amplitude histograms from three different patches containing GluA1- γ -4 fusion proteins fitted with multiple Gaussian components. The heterogeneity in observed amplitudes is apparent from the different shapes of the distributions.

Notably, when examined in heterologous cells, currents from recombinant AMPARs co-expressed with TARPs more closely resemble those from native AMPARs than

do those from AMPAR subunits expressed alone. For example, in cerebellar stellate cells, AMPAR single-channel conductance and outward rectification matches that seen

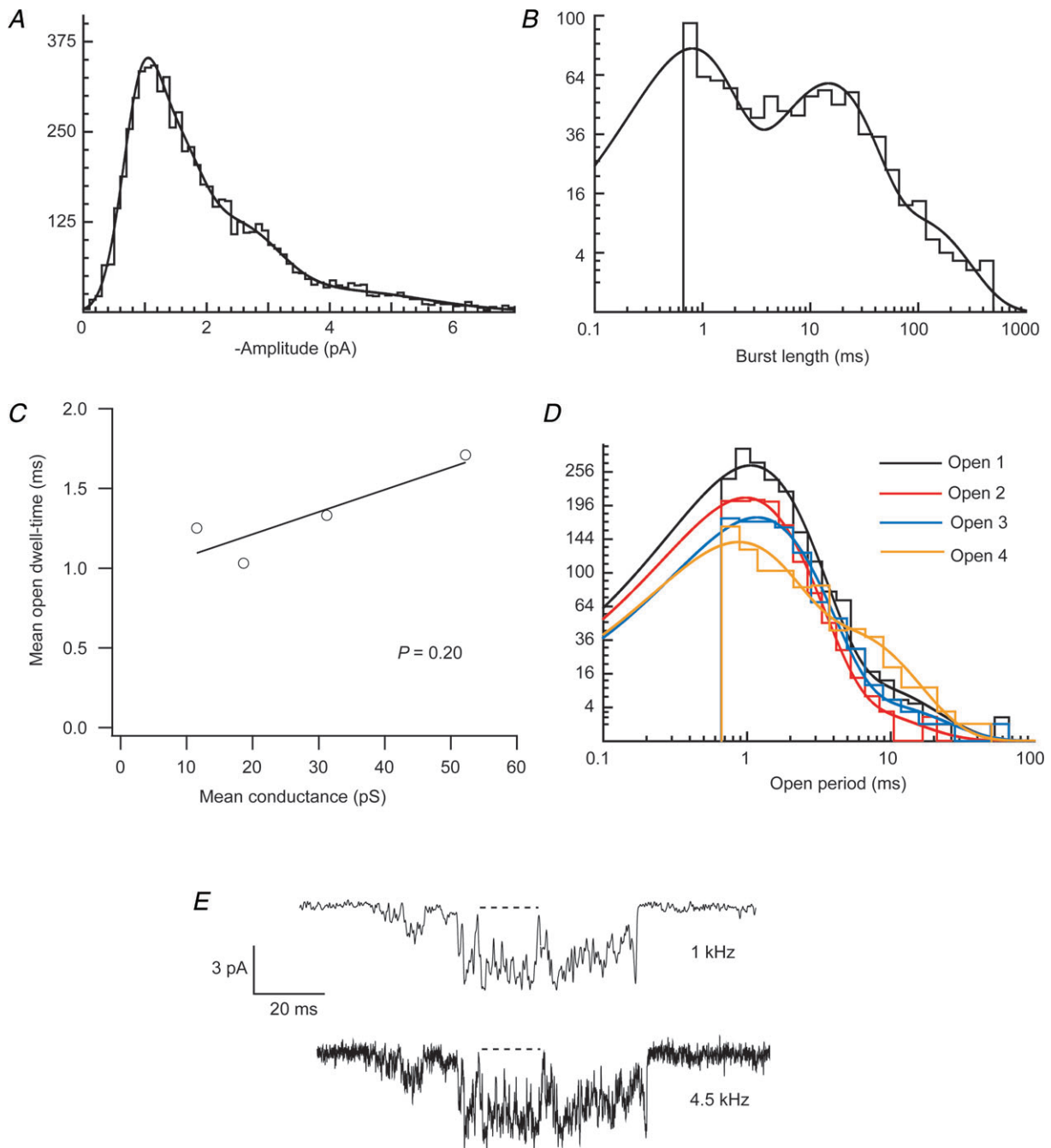


Figure 8. Pooled analysis of GluA1/γ-4 patches with similar current amplitude histograms (see Fig. 6)
A, amplitude histogram fitted with four components (see text for parameter values). *B*, burst length histogram fitted with three components (see text for parameter values). *C*, absence of significant correlation between conductance level and mean dwell-time of each conductance level. *D*, open period histograms for each conductance level required two exponential components to allow an adequate fit (see text for parameter values). *E*, open period times are 'apparent' open times, due to the imposed filtering and resolution. Reducing the filtering from 1 kHz to 4.5 kHz demonstrates that apparent open periods seen in the former condition can be interspersed with brief shutoffs when less filtering is applied; this would act to reduce the actual duration of the open period. However, the presence of these brief shutoffs would not alter the number of open period components detected.

in heterologous cells when AMPARs are coexpressed with γ -2 (Soto *et al.* 2007). Similarly, single-channel conductance, open probability and desensitisation kinetics of AMPARs in cerebellar Bergmann glial cells match those seen in heterologous cells when GluA4 is coexpressed with γ -5 (Soto *et al.* 2009). In addition, in TARP knock-out

animals, transfection of neurons to restore expression of specific TARPs restores wild type AMPAR kinetics. This has been observed for γ -2 in cerebellar granule cells (Cho *et al.* 2007; Milstein *et al.* 2007) and for γ -8 in hippocampal CA1 neurons (Shi *et al.* 2009).

We focussed our attention on GluA1 AMPARs as these are widely expressed across the CNS and as homomeric GluA1 receptors play an important role in synaptic plasticity (Kessels & Malinow, 2009). These subunits are expected to co-localise with TARPs in many brain regions due to their overlapping expression (Green *et al.* 2001; Moss *et al.* 2003; Tomita *et al.* 2003; Fukaya *et al.* 2005; Zonouzi *et al.* 2011). In addition, both γ -2 and γ -4 have been found to co-immunoprecipitate with GluA1 from cerebellar extracts (Tomita *et al.* 2003). Furthermore, these CP-AMPARs were particularly convenient and appropriate for our experiments as their conductance is large compared with that of heteromeric GluA2-containing AMPARs, a feature that is further enhanced by co-assembly with TARPs. Thus, these particular receptors allowed for a more informative and physiologically relevant analysis than was previously possible.

The number of conductance states

We detected between two and four channel conductance levels for the various GluA1/TARP combinations examined. Previous single-channel studies, carried out in the absence of auxiliary subunits, typically identified three (Swanson *et al.* 1997; Rosenmund *et al.* 1998; Jin *et al.* 2003; Fucile *et al.* 2006; Poon *et al.* 2010) or four states (Derkach *et al.* 1999; Banke *et al.* 2000; Tomita *et al.* 2005; Zhang *et al.* 2008; Prieto & Wollmuth, 2010; Kristensen *et al.* 2011). In addition to this variable number of conductance levels, a wide range of mean channel conductances – from 6 to 27 pS – has previously been described for GluA1 receptors in the absence of TARPs (Banke *et al.* 2000; Mansour *et al.* 2001; Kohda *et al.* 2003; Suzuki *et al.* 2008; Soto *et al.* 2009; Kristensen *et al.* 2011).

Why does GluA1 display up to four conductance states when associated with γ -4, but only three when associated with γ -2 or γ -5 (or in the absence of a TARP)? It may be that four levels are present in all these AMPAR assemblies but that the lowest level is not always detected because it is small, brief or rarely visited. Alternatively, as some conductance histograms differed in the number of conductance levels present, even when associated with the same TARP, it may be that not all gating ‘modes’ were sampled during all recordings. Our data suggest that the heterogeneity in the number of conductance levels of recombinant AMPARs is due to genuine intrinsic receptor variability, rather than variability in recording conditions, or the method of analysis. Such a view is

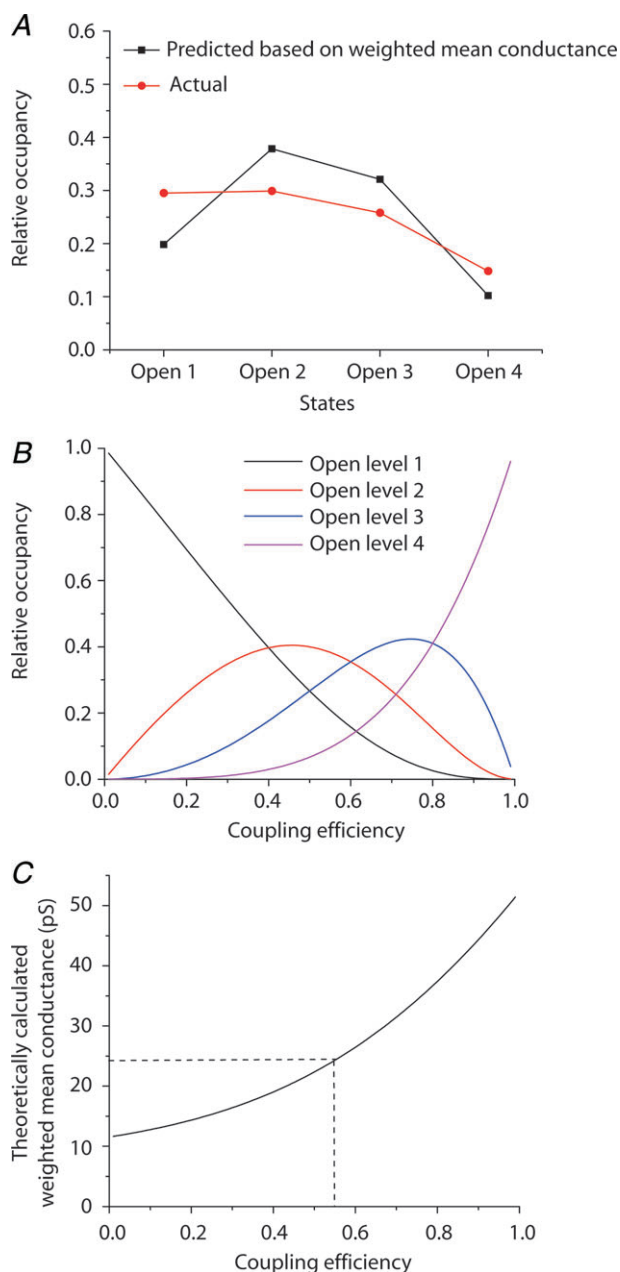


Figure 9. TARP-associated GluA1 receptors display independent subunit gating

A, occupancy of the four conductance levels (states) as measured from single-channel records and as predicted, given a subunit coupling coefficient of 0.56. B, theoretical relationship between conductance level occupancy and coupling efficiency for an independent subunit tetramer. C, the measured weighted-mean conductance predicts a coupling efficiency between subunits of 0.56.

Table 5. Comparison of conductance levels (in pS) of GluA1 receptors with and without TARPs

Conductance level	GluA1 alone					GluA1 + TARP
	Derkach <i>et al.</i> 1999 10 μ M AMPA	Banke <i>et al.</i> 2000 [†] 10 μ M glutamate	Fucile <i>et al.</i> 2006 1 μ M AMPA	Kristensen <i>et al.</i> 2011 2 mM glutamate	This study 10 mM glutamate	This study 10 mM glutamate
1	8–9**	4	***	4–5**	***	10–12*
2	12–14**	8	11	9	7.6	19–25*
3	19–21**	15	15	14–15**	12.9	37–43*
4	28–30**	25	22	21–25**	24.8	56

Each of the four conductance levels is greater in the presence of TARP, in most cases at least doubling. Although previous work utilised different agonists and agonist concentrations, the four conductance levels detected were still all lower than the highest conductance levels seen when GluA1 was coexpressed with TARPs. *Dependent on which TARP was co-expressed. **Dependent on the phosphorylation state of the receptor. ***Only three conductance levels were observed. [†]The values from Banke *et al.* 2000 were calculated as the weighted means of the conductance levels given in their fig. 6 legend.

consistent with observations made on native AMPARs in cerebellar granule cells, where between one and four conductance levels (per patch) have previously been described (Wyllie *et al.* 1993; Smith *et al.* 2000). This heterogeneity would, of course, remain undetected in studies that use fluctuation analysis to estimate mean channel conductance. Indeed, we found that estimates of weighted mean single-channel conductance were similar across the different GluA1/TARP receptor combinations, regardless of the number of conductance levels that could be directly resolved.

Potential structural or molecular factors that could give rise to the observed heterogeneity include variable GluA1/TARP stoichiometry (Shi *et al.* 2009), activity-induced dissociation of TARPs (Tomita *et al.* 2004) or variability in the phosphorylation state of GluA1 (Derkach *et al.* 1999; Kristensen *et al.* 2011). While our data demonstrate that amplitude distribution heterogeneity can still occur with the GluA1- γ -4 fusion protein, which should eliminate AMPAR/TARP stoichiometry as a source of heterogeneity, we cannot rule out that the fusion proteins are multimerising incorrectly, as observed with certain nicotinic receptors (Groot-Kormelink *et al.* 2004).

Comparison of previously reported conductance levels of GluA1 receptors expressed alone (in the present and previous studies), with our data from GluA1 receptors co-expressed with γ -4, suggests that TARP association leads to an approximate doubling in conductance of each of the sublevels and also of the maximum conductance level (Fig. 2A). Thus, the mechanism underlying the γ -4-mediated increase in channel conductance, that we observe here, differs fundamentally from that described previously for GluA4/ γ -2 assemblies (Tomita *et al.* 2005). In the earlier study, γ -2 did not significantly alter the amplitude of the subconductance levels or that of the maximum conductance, but instead increased the relative

occupancy of the largest conductance level (Tomita *et al.* 2005). Our data suggest that, rather than merely enhancing the probability that a channel will 'ratchet open' to its full conductance state, TARP γ -4 produces a more fundamental change in the receptor-channel behaviour – enhancing the amplitude of all conductance states, including the largest one.

Interestingly, while the single-channel conductance of homomeric GluA1 expressed alone (Table 5; Derkach *et al.* 1999; Banke *et al.* 2000; Fucile *et al.* 2006; Kristensen *et al.* 2011) is lower than that described for homomeric GluA4 expressed alone (Tomita *et al.* 2005), when co-expressed with a TARP both GluA1 and GluA4 exhibit similar conductance levels. One possible explanation is that GluA4 receptors are already 'optimised' to open to high-conductance levels, and that when in this condition only the proportion of high-conductance events (rather than their absolute conductance) can be increased by co-assembly with a TARP. Alternatively, it could be argued (from our data in Fig. 2A) that GluA1 receptors expressed alone have a fourth, high-conductance state that is rarely visited (and thus undetected), equivalent to the higher conductance state seen when GluA1 is coexpressed with γ -2 or γ -5. If γ -2- and γ -5-associated receptors then had a low, rarely visited (and thus undetected) conductance state, this would suggest an increased conductance mechanism similar to that of GluA4/ γ -2 rather than GluA1/ γ -4. However, previous studies on GluA1 receptors expressed alone have been able to detect four conductance levels, with the highest level being 28–30 pS (Derkach *et al.* 1999) or 21–25 pS (Kristensen *et al.* 2011). Neither of these measurements matches the highest conductance level we observe with GluA1/ γ -2 (39 pS) or GluA1/ γ -5 receptors (38 pS).

To understand better the functioning of the TARP-associated AMPARs it is useful to consider their channel activity within the constraints of a kinetic scheme,

in which each state represents a defined conformation. A complete kinetic scheme should quantitatively describe all aspects of receptor-channel functioning and allow the synaptic responses to be predicted, for any given neurotransmitter waveform. In addition, kinetic schemes allow one to visualise receptor function and to formulate hypotheses regarding states that the receptor can or cannot adopt. Potential schemes would need to take into account not only that AMPARs are tetrameric (with four glutamate binding sites), but also that the channels exhibit multiple conductance levels and desensitised states. Although it is currently difficult to accommodate all these aspects within a single scheme, and it would be premature to do so with our current data, the existence of long-lived subconductance states and multiple open dwell-time components at each conductance level places certain constraints on potential schemes. Our constraints are necessarily restricted to the open states, rather than the closed states, of the channels due to the simplifying experimental conditions that we used.

Existing data suggest that each of the open levels corresponds to varying degrees of ligation by the agonist, and hence that channel conductance is agonist concentration dependent (Rosenmund *et al.* 1998; Smith & Howe, 2000; Gebhardt & Cull-Candy, 2006). In which case, the duration of subconductance states is expected to be a function of the rate of glutamate binding plus the time interval between ligand binding and channel opening. The latter is expected to be extremely brief (in the order of 200 μ s), given the fast rise-time of AMPAR-mediated synaptic current. The duration that we observed for the long-lived subconductance states (see Fig. 5) cannot be easily explained either from the interval between binding and gating, or from the expected rate of glutamate binding to each subunit. Assuming a feasible binding rate for glutamate of $1 \times 10^8 \text{ M}^{-1} \text{ s}^{-1}$, the rate of binding to each subunit would be approximately $1 \mu\text{s}^{-1}$ for 10 mM glutamate. Interestingly, the presence of long-lived subconductance states in saturating glutamate would appear consistent with a model in which the different conductance states corresponded not to the number of bound agonist molecules, but to the number of simultaneously closed ligand-binding domains (LBDs), as has been suggested (Zhang *et al.* 2008).

The detection of two kinetically distinct open states at each conductance level for GluA1/ γ -4 receptors dictates a minimum of eight different open states in any potential kinetic scheme. Interestingly, GluA3 receptors have recently been shown to adopt two different open states at each of three conductance levels (Poon *et al.* 2010); this suggests that multiple open states per conductance level may be a general feature of AMPARs. Simple ligand binding (or LBD closure) suggests four open states. However, the number of open states in a kinetic scheme could be increased to eight if, for example, the position of

the activated subunits within the tetramer played a role. That is, if two adjacent activated subunits exhibit a kinetic profile that differs from that displayed by two diagonally opposed activated subunits. The number of open states could also be increased by explicitly separating the step of LBD closure from that of pore opening, by assuming that pore opening is not a concerted action, but instead occurs at the level of individual subunits.

It is worth noting that, if each conductance level does indeed correspond to a pore opening movement caused by a single subunit, then it is necessary to assume individual subunits each differ in their conductance contribution, to explain the fact that the steps in conductance are not all the same size, being respectively, 12, 7, 12 and 22 pS. Hence, a completely independent model – in which each subunit contributes equally to channel opening – seems highly unlikely from the present data. Although subunits may not contribute equally to channel conductance, this does not rule out the possibility that individual subunits contribute equally and independently to channel open probability. Our data are consistent with independent subunit contributions to open probability, with each subunit having a coupling coefficient of 0.56 (Fig. 9), similar to the value of 0.58 determined for GluA2 subunits in saturating glutamate (Prieto & Wollmuth, 2010). Given the symmetry observed at the level of the pore (Sobolevsky *et al.* 2009), and the independent gating of subunits, it remains an intriguing question as to how the non-additive nature of the conductance levels can arise. It would seem likely to arise from unequal steric and/or electrostatic contributions within the ion pathway that leads to the selectivity filter, which may itself arise from identical subunits adopting different tertiary structures, as has been observed with the crystal structure of GluA2 homomers (Sobolevsky *et al.* 2009).

In conclusion, our data suggest that TARPs can increase GluA1 single-channel conductance by increasing the amplitude of each of the multiple conductance levels, including the maximum channel conductance level, and that GluA1 can reside in at least two kinetically distinct open states at each conductance level.

References

- Banke TG, Bowie D, Lee H, Haganir RL, Schousboe A & Traynelis SF (2000). Control of GluR1 AMPA receptor function by cAMP-dependent protein kinase. *J Neurosci* **20**, 89–102.
- Cho CH, St-Gelais F, Zhang W, Tomta S & Howe JR (2007). Two families of TARP isoforms that have distinct effects on the kinetic properties of AMPA receptors and synaptic currents. *Neuron* **55**, 890–904.
- Collingridge GL, Olsen RW, Peters J & Spedding M (2009). A nomenclature for ligand-gated ion channels. *Neuropharmacology* **56**, 2–5.

- Colquhoun D & Sakmann B (1985). Fast events in single-channel currents activated by acetylcholine and its analogues at the frog muscle end-plate. *J Physiol* **369**, 501–557.
- Colquhoun D & Sigworth FJ (1995). Fitting and statistical analysis of single-channel records. In *Single-Channel Recording*, ed. Sakmann B & Neher E, pp. 483–587. Plenum Press, New York.
- Cull-Candy SG, Kelly L & Farrant M (2006). Regulation of Ca²⁺-permeable AMPA receptors: synaptic plasticity and beyond. *Curr Opin Neurobiol* **16**, 288–297.
- Derkach V, Barria A & Soderling TR (1999). Ca²⁺/calmodulin-kinase II enhances channel conductance of alpha-amino-3-hydroxy-5-methyl-4-isoxazolepropionate type glutamate receptors. *Proc Natl Acad Sci U S A* **96**, 3269–3274.
- Fucile S, Milei R & Eusebi F (2006). Effects of cyclothiazide on GluR1/AMPA receptors. *Proc Natl Acad Sci U S A* **103**, 2943–2947.
- Fukaya M, Yamazaki M, Sakimura K & Watanabe M (2005). Spatial diversity in gene expression for VDCCgamma subunit family in developing and adult mouse brains. *Neurosci Res* **53**, 376–383.
- Gebhardt C & Cull-Candy SG (2006). Influence of agonist concentration on AMPA and kainate channels in CA1 pyramidal cells in rat hippocampal slices. *J Physiol* **573**, 371–394.
- Gill MB, Kato AS, Wang H, Brecht DS (2012). AMPA receptor modulation by cornichon-2 dictated by transmembrane AMPA receptor regulatory protein isoform. *Eur J Neurosci* **35**, 182–194.
- Green PJ, Warre R, Hayes PD, McNaughton NC, Medhurst AD, Pangalos M, Duckworth DM & Randall AD (2001). Kinetic modification of the alpha(1) subunit-mediated T-type Ca²⁺ channel by a human neuronal Ca²⁺ channel gamma subunit. *J Physiol* **533**, 467–478.
- Groot-Kormelink PJ, Broadbent SD, Boorman JP & Sivilotti LG (2004). Incomplete incorporation of tandem subunits in recombinant neuronal nicotinic receptors. *J Gen Physiol* **123**, 697–708.
- Jackson AC & Nicoll RA (2011). The expanding social network of ionotropic glutamate receptors: TARPs and other transmembrane auxiliary subunits. *Neuron* **70**, 178–199.
- Jin R, Banke TG, Mayer ML, Traynelis SF & Gouaux E (2003). Structural basis for partial agonist action at ionotropic glutamate receptors. *Nat Neurosci* **6**, 803–810.
- Kessels HW & Malinow R (2009). Synaptic AMPA receptor plasticity and behaviour. *Neuron* **61**, 340–350.
- Kohda K, Kamiya Y, Matsuda S, Kato K, Umemori H & Yuzaki M (2003). Heteromer formation of delta2 glutamate receptors with AMPA or kainate receptors. *Brain Res Mol Brain Res* **110**, 27–37.
- Kott S, Werner M, Körber C & Hollmann M (2007). Electrophysiological properties of AMPA receptors are differentially modulated depending on the associated member of the TARP family. *J Neurosci* **27**, 3780–3789.
- Kristensen AS, Jenkins MA, Banke TG, Schousboe A, Makino Y, Johnson RC, Huganir R & Traynelis SF (2011). Mechanism of Ca²⁺/calmodulin-dependent kinase II regulation of AMPA receptor gating. *Nat Neurosci* **14**, 727–735.
- Liu SJ & Cull-Candy SG (2000). Synaptic activity at calcium-permeable AMPA receptors induces a switch in receptor subtype. *Nature* **405**, 454–458.
- Liu SJ & Zukin RS (2007). Ca²⁺-permeable AMPA receptors in synaptic plasticity and neuronal death. *Trends Neurosci* **30**, 126–134.
- Malinow R & Malenka RC (2002). AMPA receptor trafficking and synaptic plasticity. *Annu Rev Neurosci* **25**, 103–126.
- Mansour M, Nagarajan N, Nehring RB, Clements JD & Rosenmund C (2001). Heteromeric AMPA receptors assemble with a preferred subunit stoichiometry and spatial arrangement. *Neuron* **32**, 841–853.
- McManus OB & Magleby KL (1988). Kinetic states and modes of single large-conductance calcium-activated potassium channels in cultured rat skeletal muscle. *J Physiol* **402**, 79–120.
- Menuz K, O'Brien JL, Karmizadegan S, Brecht DS & Nicoll RA (2008). TARP redundancy is critical for maintaining AMPA receptor function. *J Neurosci* **28**, 8740–8746.
- Milstein AD, Zhou W, Karimzadegan S, Brecht DS & Nicoll RA (2007). TARP subtypes differentially and dose-dependently control synaptic AMPA receptor gating. *Neuron* **55**, 905–918.
- Moss FJ, Dolphin AC & Clare JJ (2003). Human neuronal stargazin-like proteins, gamma2, gamma3, and gamma4; an investigation of their specific localization in human brain and their influence on CaV2.1 voltage-dependent calcium channels expressed in *Xenopus* oocytes. *BMC Neurosci* **4**, 23.
- Poon K, Nowak LM & Oswald RE (2010). Characterizing single-channel behaviour of GluA3 receptors. *Biophys J* **99**, 14387–14446.
- Popescu G & Auerbach A (2003). Modal gating of NMDA receptors and the shape of their synaptic response. *Nat Neurosci* **6**, 476–483.
- Prieto ML & Wollmuth LP (2010). Gating modes in AMPA receptors. *J Neurosci* **30**, 4449–4459.
- Rosenmund C, Stern-Bach Y & Stevens CF (1998). The tetrameric structure of a glutamate receptor channel. *Science* **280**, 1596–1599.
- Schwenk J, Harmel N, Brechet A, Zolles G, Berkefeld H, Müller CS, Bildl W, Baehrens D, Hüber B, Kulik A, Klöcker N, Schulte U & Fakler B (2012). High-resolution proteomics unravel architecture and molecular diversity of native AMPA receptor complexes. *Neuron* **74**, 621–633.
- Schwenk J, Harmel N, Zolles G, Bildl W, Kulik A, Heimrich B, Chisaka O, Jonas P, Schulte U, Fakler B & Klöcker N (2009). Functional proteomics identify cornichon proteins as auxiliary subunits of AMPA receptors. *Science* **323**, 1313–1319.
- Shepherd JD & Huganir RL (2007). The cell biology of synaptic plasticity: AMPA receptor trafficking. *Annu Rev Cell Dev Biol* **23**, 613–643.
- Shepherd JD, Rumbaugh G, Wu J, Chowdhury S, Plath N, Kuhl D, Huganir RL & Worley PF (2006). Arc/Arg3.1 mediates homeostatic synaptic scaling of AMPA receptors. *Neuron* **52**, 475–484.

- Shi Y, Lu W, Milstein AD & Nicoll RA (2009). The stoichiometry of AMPA receptors and TARPs varies by neuronal cell type. *Neuron* **62**, 633–640.
- Smith TC & Howe JR (2000). Concentration-dependent substate behaviour of native AMPA receptors. *Nat Neurosci* **3**, 992–997.
- Smith TC, Wang LY & Howe JR (2000). Heterogeneous conductance levels of native AMPA receptors. *J Neurosci* **20**, 2073–2085.
- Sobolevsky AI, Rosconi MP & Gouaux E (2009). X-ray structure, symmetry, and mechanism of an AMPA-subtype glutamate receptor. *Nature* **462**, 745–756.
- Soto D, Coombs ID, Kelly L, Farrant M & Cull-Candy SG (2007). Stargazin attenuates intracellular polyamine block of calcium-permeable AMPA receptors. *Nat Neurosci* **10**, 1260–1267.
- Soto D, Coombs ID, Renzi M, Zonouzi M, Farrant M & Cull-Candy SG (2009). Selective regulation of long-form calcium-permeable AMPA receptors by an atypical TARP, gamma-5. *Nat Neurosci* **12**, 277–285.
- Suzuki E, Kessler M & Arai AC (2008). The fast kinetics of AMPA GluR3 receptors is selectively modulated by the TARPs gamma 4 and gamma 8. *Mol Cell Neurosci* **38**, 117–123.
- Swanson GT, Kamboj SK, Cull-Candy SG (1997). Single-channel properties of recombinant AMPA receptors depend on RNA editing, splice variation, and subunit composition. *J Neurosci* **17**, 58–69.
- Tomita S, Adesnik H, Sekiguchi M, Zhang W, Wada K, Howe JR, Nicoll RA & Brecht DS (2005). Stargazin modulates AMPA receptor gating and trafficking by distinct domains. *Nature* **435**, 1052–1058.
- Tomita S, Chen L, Kawasaki Y, Petralia RS, Wenthold RJ, Nicoll RA & Brecht DS (2003). Functional studies and distribution define a family of transmembrane AMPA receptor regulatory proteins. *J Cell Biol* **161**, 805–816.
- Tomita S, Fukata M, Nicoll RA & Brecht DS (2004). Dynamic interaction of stargazin-like TARPs with cycling AMPA receptors at synapses. *Science*, **303**, 1508–1511.
- Traynelis SF, Wollmuth LP, McBain CJ, Menniti FS, Vance KM, Ogden KK, Hansen KB, Yuan H, Myers SJ & Dingledine R (2010). Glutamate receptor ion channels: structure, regulation, and function. *Pharmacol Rev* **62**, 405–496.
- von Engelhardt J, Mack V, Sprengel R, Kavenstock N, Li KW, Stern-Bach Y, Smit AB, Seeburg PH & Monyer H (2010). CKAMP44: a brain-specific protein attenuating short-term synaptic plasticity in the dentate gyrus. *Science* **327**, 1518–1522.
- Wyllie DJ, Traynelis SF & Cull-Candy SG (1993). Evidence for more than one type of non-NMDA receptor in outside-out patches from cerebellar granule cells of the rat. *J Physiol* **463**, 193–226.
- Zhang W, Cho Y, Lolis E, Howe JR (2008). Structural and single-channel results indicate that the rates of ligand binding domain closing and opening directly impact AMPA receptor gating. *J Neurosci* **28**, 932–943.
- Zonouzi M, Renzi M, Farrant M & Cull-Candy SG (2011). Bidirectional plasticity of calcium-permeable AMPA receptors in oligodendrocyte lineage cells. *Nat Neurosci* **14**, 1430–1438.

Author contributions

C.S. performed electrophysiology experiments, data collection and analysis. All of the authors contributed to the design and interpretation of experiments. M.F. contributed to data analysis. C.S., M.F. and S.G.C.-C. wrote the paper. S.G.C.-C. and M.F. supervised the project.

Acknowledgements

We thank Dr Ian Coombs for helpful comments on the manuscript, and other members of the lab for much valuable help and discussion. S.G.C.-C. and M.F. are grateful to the Wellcome Trust and the MRC for Programme Grant support.